Nonlinear excitation of zonal flows by turbulent energy flux

Zihao Wang, Zongliang Dai,* and Shaojie Wang†
Department of Engineering and Applied Physics, University of Science and Technology of China, Hefei 230026, China

(Received 22 March 2022; accepted 19 August 2022; published 13 September 2022)

The nonlinear excitation of zonal flows (ZFs) generated by the ion-temperature-gradient turbulence in a tokamak plasma is investigated by using the global gyrokinetic code NLT. It is found that ZFs are initially driven by the nonlinear self-interaction of the eigenmode. In the nonlinear saturation, the modulational instability becomes important, and its contribution to ZFs can finally be comparable to that of the self-interaction mechanism. More importantly, both types of nonlinear wave-wave interactions can be well described by the turbulent energy flux model.

DOI: 10.1103/PhysRevE.106.035205

Zonal Flows (ZFs) [1,2] are crucially important in magnetic fusion plasma physics [3] because they regulate drift waves (DWs) [4,5] turbulence to improve the plasma confinement; it's also important in the solar atmosphere [6] and the planetary atmosphere, such as Jupiter's great red spot [7]. Many experiments [8–11] and numerical simulations [3,12] have demonstrated that ZFs can be generated spontaneously by the ion-temperature-gradient (ITG) turbulence. Understanding the nonlinear generation of ZFs is a crucial topic in fusion plasma physics and nonlinear physics.

The poloidal Reynolds stress (PRS) model [13,14] is widely used to explain the generation of the flows, which relates the poloidal flow to the nonlinear drive of PRS,

$$\partial_t \delta u_\theta = \frac{1}{nm_i}\frac{1}{r}\partial_r(r\Pi_{r\theta}),$$

where the poloidal flow $\delta u_\theta = E_r/B_T$ with E_r as the zonal radial electric field (REF) and B_T the toroidal magnetic field. $\Pi_{r\theta} = nm_i\langle\tilde{V}_r\tilde{V}_\theta\rangle_{en}$ is the radial component of the nonlinear turbulent PRS; $\tilde{V}_r$ and $\tilde{V}_\theta$ are the fluctuating components of the radial and poloidal velocities of fluid, respectively; $\langle\cdot\rangle_{en}$ denotes the turbulence ensemble average. n and m_i are the ion density and ion mass, respectively; r is the radial position. Many experimental observations have been reported [15–21] to confirm the PRS model, especially regarding the correlation between the PRS and the flows. Recent experiments on HL-2A [22] and JFT-2M [23,24] have indicated that it is the ion-pressure gradient effect rather than the PRS effect that drives the flows. The reason why the PRS effect is not important may be attributed to the neoclassical shielding of poloidal flow [25]; Rosenbluth and Hinton [26,27] found that the shielding factor $\epsilon_r \approx 1 + 1.6q^2/\sqrt{\epsilon}$ for a collisionless toroidal plasma, with q as the safety factor, and $\epsilon = r/R$ as the inverse aspect ratio; R is the major radius. This has led to the recent development of gyrokinetic theory, which predicts that zonal REF can be driven by the turbulent energy flux (TEF) [28],

$$\partial_t E_r = -\frac{1}{ne}\partial_r\left[\frac{1}{r}\partial_r\left(r\frac{2}{3}Q_r\right)\right] - B_P\frac{1}{nm_i}\frac{1}{r}\partial_r(r\Pi_{r\zeta}), \quad (1)$$

where e and B_P denote the ion charge and the poloidal magnetic field. The TEF (Q_r) and the toroidal momentum flux ($\Pi_{r\zeta}$) can be defined in the conventional way,

$$Q_r = \int d^3\boldsymbol{v}\langle\delta\dot{r}\,\delta F\rangle_{en} w, \quad (2a)$$

$$\Pi_{r\zeta} = \int d^3\boldsymbol{v}\langle\delta\dot{r}\,\delta F\rangle_{en} m_i v_\parallel \frac{B_T}{B}, \quad (2b)$$

where $\delta\dot{r}$ is the perturbation ion radial velocity and $w = \frac{1}{2}m_i v_\parallel^2 + \mu B$ is the ion kinetic energy. Here, $v_\parallel$ and μ are the parallel velocity and magnetic moment, respectively.

The above two models are from the point view of mesoscale transport. From the point view of nonlinear wave-wave interactions, the nonlinear gyrokinetic theory of modulational instability [29,30] predicts that ZFs can be readily excited via secondary modulations in the radial envelope of a single-n coherent DW (here, n is the toroidal mode number) in toroidal plasmas. The predicted modulational instability features also have been observed in three-dimensional (3D) global gyrokinetic toroidal simulations [3] of ITG modes. There, the well-developed formalism of ITG modes in toroidal geometry is given by the ballooning representation [31] with a single-n value associated with multiple-m (here, m is the poloidal mode number) harmonics due to toroidicity-induced coupling effect. Note that fluctuating fields in Ref. [29] indicate the existence of two characteristic scales for high-n DWs, namely, the eigenmode and sidebands produced by the modulation in the radial envelope. The importance of modulational instability for zonal flow excitation in the steady-state turbulence stage has been confirmed by Ref. [32]. Recent local flux-tube simulations [33] indicate that in addition to the ZF driven by modulational instability (ZFM), one can also find the ZF driven by the nonlinear self-interaction of a single-n eigenmode (ZFE). However, it is worth pointing out

*zldai@ustc.edu.cn
†wangsj@ustc.edu.cn

that such self-interaction is regarded to be a process by which an eigenmode extended along the direction parallel to the magnetic field interacts with itself nonlinearly and generate significant local ZF shear layers at radial locations near the low-order mode rational surfaces [34]. Note that these results are obtained in local simulations.

Therefore, it is of significant interest to further investigate the nonlinear generation mechanism of ZFs in global simulations. Which interaction mechanism, ZFM or ZFE, is important in the nonlinear driving of ZFs? And whether these two nonlinear wave-wave interactions are consistent with the TEF driving model?

In this article, we investigate the nonlinear excitation mechanism of ZFs through global nonlinear gyrokinetic simulations. It is found that in the quasilinear stage, it is the ZFE rather than the ZFM that is dominant; in the nonlinear saturation, the ZFM becomes important, and its contribution is eventually comparable to that of the ZFE. More importantly, ZFs either the ZFE or the ZFM can be well described by the TEF model [28].

We will focus on ITG turbulence with adiabatic electrons. The nonlinear gyrokinetic Vlasov-Poisson system is solved by using the global nonlinear gyrokinetic code NLT [35], which is based on the I-transform method [36–38]. A general and widely investigated "Cyclone DIII-D base case parameter set" [39] without collision and source is used with $R_0 = 1.6714$, $a = 0.6043$ m, and $B_0 = 1.9$ T. Here a is the minor radius of plasmas; B_0 is the magnetic field at the magnetic axis. The safety factor profile is set as

$$q(r) = 0.86 - 0.16\frac{r}{a} + 2.45\left(\frac{r}{a}\right)^2.$$

The temperature and density profile are set as

$$T(r) = T_0\exp\left[-\kappa_T\frac{a}{R_0}\Delta_T\tanh\left(\frac{(r-r_0)/a}{\Delta_T}\right)\right],$$

$$N(r) = N_0\exp\left[-\kappa_N\frac{a}{R_0}\Delta_N\tanh\left(\frac{(r-r_0)/a}{\Delta_N}\right)\right],$$

with $T_0 = 1.9693$ keV, $N_0 = 10^{19}/\mathrm{m}^3$, $\kappa_T = 6.9589$, $\kappa_N = 2.232$, $\Delta_T = \Delta_N = 0.3$, $r_0 = 0.5a$, and the normalizations of space in units of a and time in units of R_0/C_s. $\rho_* = a/\rho_i = 179$, where ρ_i is the ion thermal gyroradius. Here, $\tau = T_e/T_i = 1$ is assumed with T_i and T_e as the ion temperature and electron temperature, respectively. In these simulations, the ITG instability and ZFs evolved from a linear phase of growth to a nonlinear saturation and finally to the relaxation phase that is insensitive to initial conditions. The results are shown in Fig. 1.

The dynamic equation of zonal REF, Eq. (1), is examined for the above full-n simulations. Different contributions of Q_r and $\Pi_{r\zeta}$ to zonal REF in the early nonlinear saturation and in the steady-state turbulence stage are shown in Figs. 2(a) and 2(b), respectively. It can be clearly seen that in both stages, the turbulent energy flux is quite important for the nonlinear drive of ZFs. The radial structure of TEF, determined by the turbulent morphology, is in agreement with the structure of zonal REF, in terms of both the mesoscopic scale and the amplitude. Zonal REF presented in Fig. 2(b) shown in typical mesoscale radial structure, which is larger than the spatial

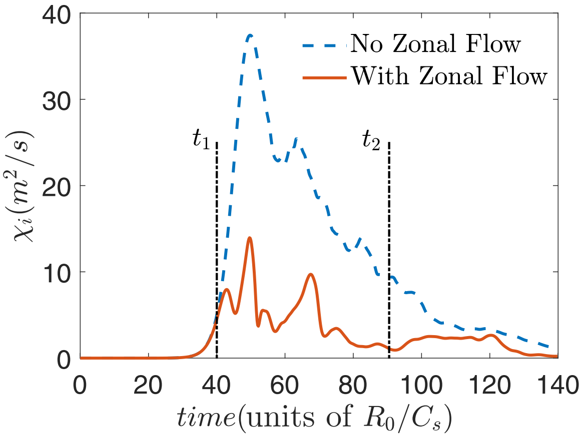

FIG. 1. Time history of turbulent ion thermal conductivities χ_i at $r = 0.45a$ with (solid) and without (dashed) zonal flows by using NLT with plasma parameters in Ref. [39]. R_0 and $C_s = \sqrt{T_i/m_i}$ are the major radius in the magnetic axis and ion sound speed, respectively.

scale of turbulence but smaller than the equilibrium scale. However, the scale of zonal REF shown in Fig. 2(a) is not well separated from the equilibrium scale. This will be discussed further later.

The full-n simulation shown in Fig. 1 demonstrates that ZFs, which are already excited in the quasilinear stage, significantly reduce the turbulent ion thermal conductivity χ_i in nonlinear saturation. This result is consistent with the observation of Lin's early 3D global gyrokinetic simulations [3]. This indicates that in the quasilinear stage, ZFs have reduced DWs and influenced its saturation process. Therefore, it is

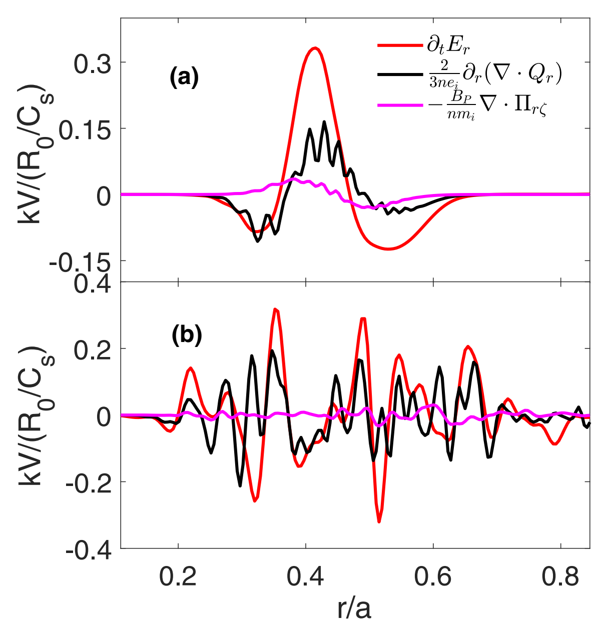

FIG. 2. Test of Eq. (1) for the nonlinear full-n case at (a) the early nonlinear saturation ($t_1 = 40R_0/C_s$) and (b) the steady-state turbulence stage ($t_2 = 90R_0/C_s$ marked in Fig. 1). The zonal REF term (solid), TEF term (dotted), and toroidal momentum flux term (dashed) are normalized by $\mathrm{kV}/(R_0/C_s)$.

important to analyze the excitation mechanism of ZFs driven by nonlinear wave-wave interactions in the quasilinear stage.

Following the two types of interaction models in Refs. [29,33], we consider a single-n (the most unstable mode $n = \pm 18$) DW and ZFs system. The perturbation distribution function is written as

$$\delta f = \delta f_{+n} e^{in\zeta} + \delta f_{-n} e^{-in\zeta} + \delta f_z, \tag{3}$$

where the subscript z denotes the $n = 0$ Fourier component; ζ is the toroidal angle. The equilibrium distribution F_0 is chosen as a local Maxwellian.

First, we have carried out the standard nonlinear case, which is described as follows. Define

$$\mathcal{L}(\delta f) = \partial_t \delta f + \dot{\boldsymbol{X}}_0 \cdot \nabla \delta f + \dot{v}_{\parallel,0} \partial_{v_\parallel} \delta f, \tag{4}$$

where $\dot{\boldsymbol{X}}_0$ and $\dot{v}_{\parallel,0}$ are unperturbed guiding-center velocity and parallel acceleration, respectively. The evolution equations describing the perturbation distribution function can be written as

$$\underbrace{\mathcal{L}(\delta f_n) + \{\delta\phi_n, F_0\}}_{\text{linear response}} + \underbrace{\{\delta\phi_n, \delta f_z\}}_{\text{N.F.}} + \underbrace{\{\delta\phi_z, \delta f_n\}}_{\text{modulation}} = 0; \tag{5}$$

$$\underbrace{\mathcal{L}(\delta f_z) + \{\delta\phi_z, F_0\}}_{\text{linear response}} + \underbrace{\{\delta\phi_z, \delta f_z\}}_{\text{N.F.}} + \underbrace{\{\delta\phi_{-n}, \delta f_n\} + \{\delta\phi_n, \delta f_{-n}\}}_{\text{nonlinear driving}} = 0, \tag{6}$$

where $\{,\}$ denotes the unperturbed Poisson's bracket; "N. F." denotes the nonlinear flattening effects. The Fourier component $\delta\phi_n$ in Eq. (5) contains both the eigenmode and the sidebands discussed in Ref. [29]. Thus, the nonlinear driving term in Eq. (6) contains both envelope modulation interactions (if the two subscripts are viewed as eigenmodes and sidebands, respectively) and eigenmode self-interactions (if both subscripts are viewed as eigenmodes). On the other hand, the nonlinear driving term in Eq. (6) clearly represents the ensemble averaged turbulent transport flux which has been discussed in Ref. [28].

In order to separate out the modulational instability and the self-interaction of the eigenmode, we have carried out another case: the modulation-off case. We only retain the linear term in Eq. (5), but Eq. (6) for ZFs is unchanged. Clearly, the DW in the second case is simply the eigenmode; it does not contain the sidebands, hence, the ZFE is well separated out by closing the feedback loop of ZFs to the DW.

The modulational instability in the standard nonlinear case is obtained by the Gram-Schmidt orthogonal method. Specifically, the radial envelope of DW takes

$$\delta\Phi_{\text{env}}(r) = \langle\sqrt{\delta\phi_{+n}(r,\theta)\delta\phi_{-n}(r,\theta)}\rangle_\theta. \tag{7}$$

Thus, the radial envelope of sidebands $\delta\Phi_s(r)$ is found by using the radial envelope of eigenmode $\delta\Phi_e(r)$ derived from the modulation-off case and the radial envelope of DWs $\delta\phi_d(r)$ in the standard nonlinear case,

$$\delta\Phi_s(r) = \delta\phi_d(r) - \delta\Phi_e(r)\langle\delta\phi_d, \delta\Phi_e\rangle_{ip}/\langle\delta\Phi_e, \delta\Phi_e\rangle_{ip}. \tag{8}$$

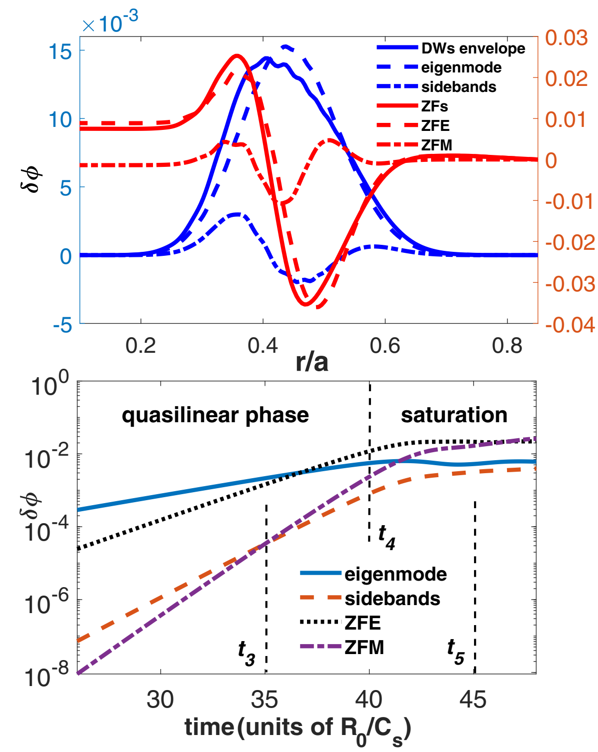

FIG. 3. (a) The orthogonal decomposed radial structure of the DWs envelope and ZFs at the early nonlinear saturation $t_4 = 40R_0/C_s$ [marked in Fig. 3(b)], normalized by the equilibrium temperature. (b) The temporal evolution of the potential of four components: $\delta\phi_e$ (solid line), $\delta\phi_s$ (dashed line), $\delta\phi_{ze}$ (dotted line), and $\delta\phi_{zm}$ (dashed-dot line) in the quasilinear phase and nonlinear saturation.

Using these functional bases to orthogonalize the DWs envelope in the standard nonlinear case, we found

$$\delta\phi_d(r,t) = k_e(t)\delta\Phi_e(r) + k_s(t)\delta\Phi_s(r), \tag{9a}$$

$$k_e(t) = \langle\delta\phi_d, \delta\Phi_e\rangle_{ip}/\langle\delta\Phi_e, \delta\Phi_e\rangle_{ip}, \tag{9b}$$

$$k_s(t) = \langle\delta\phi_d, \delta\Phi_s\rangle_{ip}/\langle\delta\Phi_s, \delta\Phi_s\rangle_{ip}. \tag{9c}$$

The inner product is defined as $\langle f, g\rangle_{ip} = \int_a^b f(r)g(r)dr$ with a and b as the lower and upper bounds of integral determined by the turbulence development region.

The same orthogonal decomposition can be performed to ZFs in the standard nonlinear case $\delta\phi_z$ to separate the ZFE $\delta\Phi_{ze}$ from the ZFM $\delta\Phi_{zm}$,

$$\delta\phi_z(r,t) = k_{ze}(t)\delta\Phi_{ze}(r) + k_{zm}(t)\delta\Phi_{zm}(r). \tag{10}$$

Note that $\delta\Phi_{ze}(r)$ is derived from the modulation-off case. The decomposition results of the DWs envelope and radial structure of ZFs in early nonlinear saturation $t_4 = 40R_0/C_s$ are shown in Fig. 3(a). And the temporal evolution of different components [$k_e(t)$, $k_s(t)$, $k_{ze}(t)$, and $k_{zm}(t)$] is shown in Fig. 3(b).

We find that the radial structure of ZFs in Fig. 3(a) is similar to that (i.e., $\partial_t E_r$) in Fig. 2(a). The reason is that the $n = 18$ mode picked in the above single-n simulation is the most unstable one in the full-n simulation; it is dominant in the early nonlinear saturation in the full-n simulation. Note that the scale of turbulence envelope of the $n = 18$ mode is usually taken as mesoscale. However, in realistic simulations, as is shown in Fig 3(a), the scale of the turbulence envelope is not well separated from the equilibrium scale. This explains why the scale of ZFs shown in Figs. 2(a) and 3(a) is not well separated from the equilibrium scale.

Growth rates of the eigencomponent of DW (γ_e), the ZFE (γ_{ze}), the sidebands (γ_s), and the ZFM (γ_{zm}) can be readily found from Fig. 3(b). In the quasilinear stage, one finds the following simple relations: $\gamma_e = \gamma_L \approx 0.218 C_s/R_0$,

$$\gamma_{ze} = \gamma_e + \gamma_e = 2\gamma_e, \tag{11}$$

$$\gamma_s = \gamma_e + \gamma_{ze} = 3\gamma_e, \tag{12}$$

$$\gamma_{zm} = \gamma_e + \gamma_s = 4\gamma_e. \tag{13}$$

These simple relations reflect the usual nonlinear coupling physics and can be easily understood by examining the nonlinearity in Eqs. (5) and (6). If the eigenmode is taken as a first-order perturbation, then it can be found that the ZFE is a second-order nonlinear effect and the sidebands and the ZFM can be further viewed as third- and fourth-order effects; this explains the simple $N\gamma_e$ relations. These hierarchical wave-wave interactions can also be "felt" in their progressively finer radial structure, such as the number of peaks and valleys shown in Fig. 3(a).

Equations (12) and (13) indicate that the growth rates of the sidebands and ZFM are independent of the amplitude of the eigenmode, which is different from the modulational instability discussed in Ref. [29]; here the sidebands is excited by the modulation of ZFE rather than ZFM itself [29]. Clearly, the ZFM here is indeed driven by the envelope modulation, but it is not driven by the modulational instability [29].

The above simple multiplicity relations is maintained until $t_4 \approx 40R_0/C_s$, i.e., the early nonlinear saturation. After that, the simple relations that apply to quasilinear stage are broken. In the nonlinear saturation, such as $t_5 \approx 45R_0/C_s$ from Fig. 3(b), one can find that $\gamma_e \approx 0$, $\gamma_{ze} \approx 0$, thus, the ZFE (black dotted line) is no longer growing. On the other hand, $\gamma_e \approx 0$ leads to $\gamma_s = \gamma_e + \gamma_{zm} = \gamma_{zm}$ and $\gamma_{zm} = \gamma_e + \gamma_s = \gamma_s$, which can be clearly seen from the slope or growth rate of sidebands and of ZFM after $t > 42R_0/C_s$ in Fig. 3(b); this indicates that in the nonlinear saturation, the ZFM is driven by the modulational instability [29,32] as the eigencomponent of DWs stops growing, which is consistent with Ref. [29].

It should be emphasized that in Fig. 3(b), when $t < 40R_0/C_s$, $\gamma_{zm} = \gamma_e + \gamma_s > \gamma_s$, thus, the ZFM is not driven by the modulational instability [29,32], which has been extensively discussed above. However, when $t > 42R_0/C_s$, $\gamma_{zm} = \gamma_s$, the ZFM is indeed driven by the modulational instability [29,32].

As can be seen in Fig. 3(b), the intensity of ZFE is clearly much larger than that of ZFM from the quasilinear stage to the early nonlinear saturation. This clearly demonstrated that the ZFE, which is excited by the self-interaction of the eigenmode, is dominant in the quasilinear stage. Although the growth rate of ZFM is large, the envelope modulation is not important in quasilinear stage. Therefore, the growth behavior of ZFs in the quasilinear stage can be described by the self-interaction of the eigenmode.

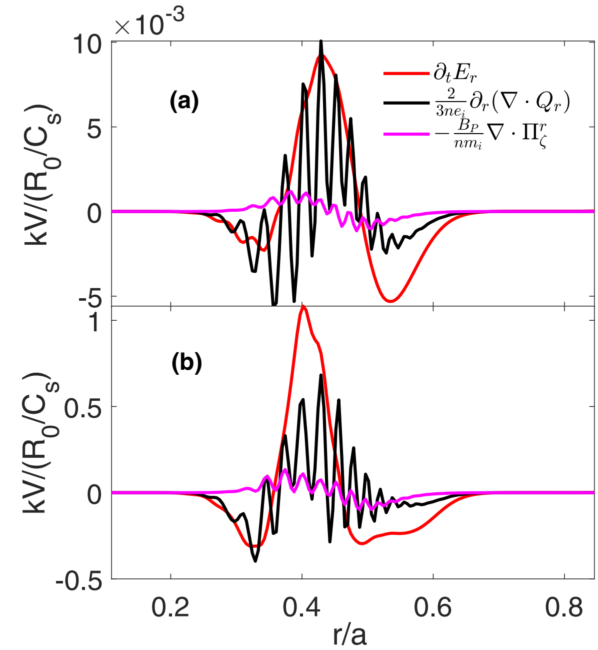

FIG. 4. The test of Eq. (1) for the nonlinear single-n case at (a) the quasilinear stage ($t_3 = 35R_0/C_s$) and (b) the nonlinear saturation [$t_5 = 45R_0/C_s$ marked in Fig. 3(b)]. The zonal REF term (solid), TEF term (dotted), and toroidal momentum flux term (dashed) are normalized by $kV/(R_0/C_s)$.

However, an important observation from Fig. 3(b) is that the amplitudes of ZFE and ZFM are comparable to each other in the nonlinear saturation, so neither can be neglected. This result was obtained in our global simulations, which is different from the local flux-tube simulations [33]. It should be particularly noted that the self-interaction of the eigenmode discussed in this paper is the nonlinear self-interaction of the global microinstability eigenmode rather than local. This self-interaction treats n of the eigenmode as the unique quantum number without distinguishing the specific m, and is, therefore, not the same as the self-interaction in Ref. [33] that needs to distinguish different harmonics.

It should be pointed out that the above discussion on the relative importance of the ZFE and ZFM is based on single-n simulations. Note that it is shown in Fig. 3(b) when the single-n ITG mode is saturated ($t > 42R_0/C_s$), and the modulational instability [29,32] is important. This observation is based on Gram-Schmidt orthogonalization decomposition. It's difficult to extend this decomposition method to the steady-state turbulence stage especially for the full-n case. We note that in the steady-stage turbulence stage, the importance of modulational instability has been clearly confirmed in Ref. [32].

Test of the TEF model for the single-n DW-ZFs system is shown in Fig. 4, which indicates that the contribution of TEF to ZFs is significant in both the quasilinear stage and the nonlinear saturation. This finding does not differ much from the full-n condition. Therefore, the TEF model can well describe the evolution of ZFs from the linear stage of turbulence to the nonlinear saturation.

In conclusion, the nonlinear excitation of ZFs by the ITG turbulence in a tokamak plasma is investigated by using the global gyrokinetic code NLT. We find that the ZFE, or the self-interaction of the eigenmode, dominates in the quasilinear stage; the ZFM, or modulational instability [29,32], becomes important and eventually comparable to the ZFE in the nonlinear saturation stage. Furthermore, we point out that ZFs both the ZFE and the ZFM, are well described by the TEF model [28] in both the quasilinear stage and the steady-state stage, which is consistent with recent experiments [22–24]. The debate on the driving of ZFs by poloidal Reynolds stress in different experiments and simulations is subject to further work.

This work was supported by the National Natural Science Foundation of China (Grants Nos. 12075240 and 11875254), and the National MCF Energy R&D Program of China (Grant No. 2019YFE03060000).

[1] A. Hasegawa and M. Wakatani, Phys. Rev. Lett. **59**, 1581 (1987).
[2] P. H. Diamond, S. Itoh, K. Itoh, and T. Hahm, Plasma Phys. Controlled Fusion **47**, R35 (2005).
[3] Z. Lin, T. S. Hahm, W. Lee, W. M. Tang, and R. B. White, Science **281**, 1835 (1998).
[4] W. Horton, Rev. Mod. Phys. **71**, 735 (1999).
[5] T. Hahm, M. Beer, Z. Lin, G. Hammett, W. Lee, and W. Tang, Phys. Plasmas **6**, 922 (1999).
[6] G. Rudiger and G. Rüdiger, *Differential Rotation and Stellar Convection: Sun and Solar-Type Stars* (Gordon and Breach Science Publishers, 1989).
[7] A. P. Ingersoll, R. F. Beebe, J. L. Mitchell, G. W. Garneau, G. M. Yagi, and J.-P. Müller, J. Geophys. Res.: Space Phys. **86**, 8733 (1981).
[8] A. Fujisawa, K. Itoh, H. Iguchi, K. Matsuoka, S. Okamura, A. Shimizu, T. Minami, Y. Yoshimura, K. Nagaoka, C. Takahashi, M. Kojima, H. Nakano, S. Ohsima, S. Nishimura, M. Isobe, C. Suzuki, T. Akiyama, K. Ida, K. Toi, S. I. Itoh *et al.*, Phys. Rev. Lett. **93**, 165002 (2004).
[9] D. K. Gupta, R. J. Fonck, G. R McKee, D. J. Schlossberg, and M. W. Shafer, Phys. Rev. Lett. **97**, 125002 (2006).
[10] S. Coda, M. Porkolab, and K. H. Burrell, Phys. Rev. Lett. **86**, 4835 (2001).
[11] G. S. Xu, B. N. Wan, M. Song, and J. Li, Phys. Rev. Lett. **91**, 125001 (2003).
[12] A. M. Dimits, T. J. Williams, J. A. Byers, and B. I. Cohen, Phys. Rev. Lett. **77**, 71 (1996).
[13] P. Diamond and Y.-B. Kim, Phys. Fluids B **3**, 1626 (1991).
[14] P. H. Diamond, Y.-M. Liang, B. A. Carreras, and P. W. Terry, Phys. Rev. Lett. **72**, 2565 (1994).
[15] C. Hidalgo, M. Pedrosa, E. Sánchez, R. Balbín, A. López-Fraguas, B. Van Milligen, C. Silva, H. Fernandes, C. Varandas, C. Riccardi *et al.*, Plasma Phys. Controlled Fusion **42**, A153 (2000).
[16] Y. H. Xu, C. X. Yu, J. R. Luo, J. S. Mao, B. H. Liu, J. G. Li, B. N. Wan, and Y. X. Wan, Phys. Rev. Lett. **84**, 3867 (2000).
[17] T. Estrada, T. Happel, C. Hidalgo, E. Ascasibar, and E. Blanco, Europhys. Lett. **92**, 35001 (2010).
[18] G. D. Conway, C. Angioni, F. Ryter, P. Sauter, and J. Vicente, Phys. Rev. Lett. **106**, 065001 (2011).
[19] G. S. Xu, B. N. Wan, H. Q. Wang, H. Y. Guo, H. L. Zhao, A. D. Liu, V. Naulin, P. H. Diamond, G. R. Tynan, M. Xu, R. Chen, M. Jiang, P. Liu, N. Yan, W. Zhang, L. Wang, S. C. Liu, S. Y. Ding, Phys. Rev. Lett. **107**, 125001 (2011).
[20] L. Schmitz, L. Zeng, T. L. Rhodes, J. C. Hillesheim, E. J. Doyle, R. J. Groebner, W. A. Peebles, K. H. Burrell, and G. Wang, Phys. Rev. Lett. **108**, 155002 (2012).
[21] G. Tynan, M. Xu, P. Diamond, J. Boedo, I. Cziegler, N. Fedorczak, P. Manz, K. Miki, S. Thakur, L. Schmitz *et al.*, Nucl. Fusion **53**, 073053 (2013).
[22] J. Cheng, J. Q. Dong, K. Itoh, L. W. Yan, M. Xu, K. J. Zhao, W. Y. Hong, Z. H. Huang, X. Q. Ji, W. L. Zhong, D. L. Yu, S. I. Itoh, L. Nie, D. F. Kong, T. Lan, A. D. Liu, X. L. Zou, Q. W. Yang, X. T. Ding, X. R. Duan *et al.*, Phys. Rev. Lett. **110**, 265002 (2013).
[23] T. Kobayashi, K. Itoh, T. Ido, K. Kamiya, S.-I. Itoh, Y. Miura, Y. Nagashima, A. Fujisawa, S. Inagaki, K. Ida, K. Hoshino, Phys. Rev. Lett. **111**, 035002 (2013).
[24] T. Kobayashi, K. Itoh, T. Ido, K. Kamiya, S.-I. Itoh, Y. Miura, Y. Nagashima, A. Fujisawa, S. Inagaki, K. Ida *et al.*, Nucl. Fusion **54**, 073017 (2014).
[25] K. Itoh and S.-I. Itoh, Plasma Phys. Controlled Fusion **38**, 1 (1996).
[26] M. N. Rosenbluth and F. L. Hinton, Phys. Rev. Lett. **80**, 724 (1998).
[27] F. Hinton and M. Rosenbluth, Plasma Phys. Controlled Fusion **41**, A653 (1999).
[28] S. Wang, Phys. Plasmas **24**, 102508 (2017).
[29] L. Chen, Z. Lin, and R. White, Phys. Plasmas **7**, 3129 (2000).
[30] L. Chen, R. B. White, and F. Zonca, Phys. Rev. Lett. **92**, 075004 (2004).
[31] J. W. Connor, R. Hastie, and J. B. Taylor, Proc. R. Soc. A **365**, 1 (1979).
[32] P. Diamond, S. Champeaux, M. Malkov, A. Das, I. Gruzinov, M. Rosenbluth, C. Holland, B. Wecht, A. Smolyakov, F. Hinton *et al.*, Nucl. Fusion **41**, 1067 (2001).
[33] C. Ajay, S. Brunner, B. McMillan, J. Ball, J. Dominski, and G. Merlo, J. Plasma Phys. **86**, 905860504 (2020).
[34] A. Weikl, A. Peeters, F. Rath, F. Seiferling, R. Buchholz, S. Grosshauser, and D. Strintzi, Phys. Plasmas **25**, 072305 (2018).
[35] L. Ye, Y. Xu, X. Xiao, Z. Dai, and S. Wang, J. Comput. Phys. **316**, 180 (2016).
[36] S. Wang, Phys. Plasmas **19**, 062504 (2012).
[37] S. Wang, Phys. Rev. E **87**, 063103 (2013).
[38] S. Wang, Phys. Plasmas **20**, 082312 (2013).
[39] A. M. Dimits, G. Bateman, M. Beer, B. Cohen, W. Dorland, G. Hammett, C. Kim, J. Kinsey, M. Kotschenreuther, A. Kritz *et al.*, Phys. Plasmas **7**, 969 (2000).